

# Nonperturbative Higgs propagator: NLO correction in the $1/N$ expansion

A. Ghinculov<sup>1</sup>, T. Binoth and J.J. van der Bij

*Albert–Ludwigs–Universität Freiburg, Fakultät für Physik  
Hermann–Herder Str.3, D-79104 Freiburg, Germany*

## Abstract

We derive a nonperturbative result for the Higgs propagator by calculating the NLO correction in the  $1/N$  expansion of  $O(N)$  sigma models. For dealing with the  $1/N$  expansion beyond leading order, we develop techniques to calculate certain infinite sets of multiloop Feynman diagrams. We then calculate the Higgs lineshape in fermion scattering, as seen for instance at a muon collider. We compare with the existing two-loop perturbative results. There is a considerable discrepancy between perturbation theory and the  $1/N$  expansion in LO. By including the NLO correction, this discrepancy is reduced dramatically. The results are in very good agreement with the two-loop result even for masses as high as 850 GeV. A maximum of the mass is reached at 930 GeV. For phenomenological purposes, we give a simple approximate relation between the Higgs mass and width.

---

<sup>1</sup>Address after October 1, 1997: Randall Laboratory of Physics, University of Michigan, Ann Arbor, Michigan 48109–1120, USA

# Nonperturbative Higgs propagator: NLO correction in the $1/N$ expansion

A. Ghinculov<sup>†</sup>, T. Binoth and J.J. van der Bij

*Albert-Ludwigs-Universität Freiburg, Fakultät für Physik,  
Hermann-Herder Str.3, D-79104 Freiburg, Germany*

## Abstract

We derive a nonperturbative result for the Higgs propagator by calculating the NLO correction in the  $1/N$  expansion of  $O(N)$  sigma models. For dealing with the  $1/N$  expansion beyond leading order, we develop techniques to calculate certain infinite sets of multiloop Feynman diagrams. We then calculate the Higgs lineshape in fermion scattering, as seen for instance at a muon collider. We compare with the existing two-loop perturbative results. There is a considerable discrepancy between perturbation theory and the  $1/N$  expansion in LO. By including the NLO correction, this discrepancy is reduced dramatically. The results are in very good agreement with the two-loop result even for masses as high as 850 GeV. A maximum of the mass is reached at 930 GeV. For phenomenological purposes, we give a simple approximate relation between the Higgs mass and width.

## 1 Introduction

With the discovery of the vector bosons and of the top quark behind us, the next major question in the phenomenology of the weak interactions is the search for the Higgs boson. Within the standard model the properties of the Higgs boson are determined when its mass is fixed, as the tree level selfcouplings are proportional to  $m_H^2$ . As long as the Higgs particle is light, there are no fundamental problems in determining its properties from perturbation theory. However, when the Higgs particle becomes heavy,  $\mathcal{O}(TeV)$ , the selfcoupling becomes large, and perturbation theory becomes unreliable.

Therefore one would like to find an approximation to Higgs physics beyond perturbation theory which is applicable for large couplings as well. When one realizes that

---

<sup>†</sup>Address after October 1, 1997: Randall Laboratory of Physics, University of Michigan, Ann Arbor, Michigan 48109-1120, USA

the Higgs sector of the standard model is nothing but an  $O(4)$  linear sigma model, the expansion in  $1/N$  of the  $O(N)$ -symmetric sigma model suggests itself.

The  $1/N$  expansion has a long history [1]–[11], and has also been applied to the Higgs boson of the standard model [1, 2]. The results in leading order in  $1/N$  are interesting. They indicate a saturation of the Higgs boson mass when the coupling increases. Also the relation between the Higgs width and mass is very different at larger couplings. However, the situation at leading order is not satisfactory because the lowest order is numerically very far from perturbation theory for small Higgs mass. Perturbation theory has recently even been extended to the two-loop level [12, 13, 14], and should be well under control for small Higgs mass. This shed for a long time doubts on the relevance of the  $1/N$  approach. In order to clarify the situation it is therefore clearly desirable to know the next-to-leading order contribution in  $1/N$ .

What makes the  $1/N$  expansion particularly interesting is that it has certain features which are absent in perturbation theory, and which are to be expected from an exact solution. One feature is the absence in physical results of any renormalization scheme dependence. As we shall see, the next-to-leading order solution which we will derive has another such feature, namely the finiteness of wave function renormalization constants. Interestingly enough, this occurs after the summation of Feynman diagrams which are all ultraviolet divergent.

The  $O(N)$  sigma model at leading order in the  $1/N$  expansion was discussed in detail by a number of authors. These works study the effective potential and the question of the occurrence of spontaneous symmetry breaking in  $O(N)$  models, as well as two- and four-point Green functions. These aspects were studied from two points of view. One attempts to treat the  $O(N)$  sigma model as a fundamental, renormalized theory; and the other as an effective theory, with a built-in cutoff. Although a large amount of work was done, most of it is limited to the leading order. Root [8] wrote down expressions for the effective potential in higher order, but did not evaluate them explicitly. The reason for this is twofold. First of all, the expressions are quite complicated. More fundamental is the occurrence of a tachyon in the theory.

A striking feature of the leading order solution is the presence in the propagators of a tachyonic pole. As long as one is concerned only with the leading order, and the Higgs coupling is not very strong, the causality violating effects induced by the tachyon are at least numerically negligible. They are suppressed essentially by the Landau scale. However, if one wants to calculate higher order corrections, these effects are unavoidable because the tachyon appears then in loops and leads to pathological solutions. For instance, it was shown by Root [8] that the effective potential becomes complex in next-to-leading order.

The tachyon problem is similar to the Landau ghost in perturbation theory. However, the occurrence and position of the Landau ghost relies on using a perturbative expression precisely where one knows this expression is not a good approximation anymore. For the case of the tachyon problem in the  $1/N$  expansion this is no more the case. The propagators in the  $1/N$  expansion are summed to all orders in the

coupling constant. Thus their validity does not depend on the strength of the coupling. A possible interpretation for the presence of the tachyon is that it indicates the triviality of the theory.

One simple and consistent way to deal with the tachyon is to regard the  $O(N)$  model as an effective theory and to introduce explicitly a cutoff under the tachyon scale [3]. However, we prefer to use in this paper a different approach. We introduce a scheme to subtract minimally the tachyon from the Green functions order by order in the  $1/N$  expansion. This procedure is well-adapted to the calculation of higher order effects in  $1/N$ .

The outline of this paper is the following. In section 2 we introduce the model and the leading order for fixing the notations. In the following section we discuss and motivate in detail the prescription for the treatment of the tachyon problem. In section 4 we describe the next-to-leading order calculation and the methods for evaluating the multiloop diagrams involved. In section 5 we treat the Higgs lineshape nonperturbatively and discuss the results. Section 6 summarizes the conclusions of the paper.

## 2 Renormalization and leading order solution

The  $O(N)$  sigma model at leading order in the  $1/N$  expansion was already discussed extensively in the literature. For this reason, we will not repeat here this discussion. In the following, for fixing the notations, we will only derive the two-point functions, assuming that the theory has a ground state with spontaneously broken symmetry.

The starting point of the calculation is the following Lagrangian:

$$\mathcal{L} = \frac{1}{2} \partial_\nu \Phi_0 \partial^\nu \Phi_0 - \frac{\mu_0^2}{2} \Phi_0^2 - \frac{\lambda_0}{4!N} \Phi_0^4 \quad (1)$$

Here  $\Phi$  is a scalar field with  $N$  components  $\phi^i$ ,  $i = 1, \dots, N$ . In principle one could use this Lagrangian in order to calculate contributions in different orders of  $1/N$ . However, the combinatorics becomes very complicated and it is advantageous to introduce an auxiliary field  $\chi$ , and add a nondynamical term to the Lagrangian according to a combinatorial trick proposed in ref. [11]:

$$\begin{aligned} \mathcal{L} &= \mathcal{L} + \frac{3N}{2\lambda_0} \left( \chi_0 - \frac{\lambda_0}{6N} \Phi_0^2 - \mu_0^2 \right)^2 \\ &= \frac{1}{2} \partial_\nu \Phi_0 \partial^\nu \Phi_0 - \frac{1}{2} \chi_0 \Phi_0^2 + \frac{3N}{2\lambda_0} \chi_0^2 - \frac{3\mu_0^2 N}{\lambda_0} \chi_0 + \text{const.} \end{aligned} \quad (2)$$

This form of the Lagrangian has the same physical content as before. However, the Feynman rules are changed, thereby facilitating the counting of powers of  $1/N$ . For doing higher order calculations, the introduction of the extra field  $\chi$  is practically the only way not to get lost in the combinatorics – see also ref. [8].

The fields and coupling constants in eqns. 1, 2 are bare quantities. In order to perform renormalization, we make the following substitutions:

$$\frac{3}{\lambda_0} = \frac{3}{\lambda} + \Delta\lambda \quad (3)$$

$$\frac{3\mu_0}{\lambda_0} = -\frac{v^2}{2}(1 + \Delta t_\sigma) \quad (4)$$

$$\phi_i^0 = \pi_i Z_\pi \quad , \quad i = 1, \dots, N-1 \quad (5)$$

$$\phi_N^0 = \sigma Z_\sigma + \sqrt{N}v \quad (6)$$

$$\chi^0 = \chi Z_\chi + \hat{\chi} + \Delta t_\chi \quad (7)$$

Here  $\sqrt{N}v$  and  $\hat{\chi}$  are the expectation values of the fields  $\Phi$  and  $\chi$  in the broken symmetry ground state. For the case of the standard model Higgs sector,  $N = 4$  and  $v = 123$  GeV.  $\Delta t_\sigma$  and  $\Delta t_\chi$  are the tadpole counterterms corresponding to the fields  $\sigma$  and  $\chi$ .

The tadpole counterterms  $\Delta t_\sigma$  and  $\Delta t_\chi$  can be determined in the following way. In the original Lagrangian of eq. 1 only one tadpole counterterm is needed. Upon introduction of the auxiliary field  $\chi$  two such counterterms are present, but they are related to each other. Some contributions can be shifted from the definition of one counterterm to the other. It is then convenient for performing a next-to-leading order calculation to define the tadpole counterterms so that the vacuum expectation values of the fields  $\sigma$  and  $\chi$  do not receive corrections in higher orders. By solving the gap equation in leading order, it is well-known that one finds in the broken symmetry ground state  $\hat{\chi} = 0$ . By requesting that this simple relation be preserved in higher orders, we fix uniquely the relation between the two tadpole counterterms  $\Delta t_\sigma$  and  $\Delta t_\chi$ . Therefore, we define  $\Delta t_\sigma$  and  $\Delta t_\chi$  by the condition that the one-point functions for the fields  $\sigma$  and  $\chi$  vanish. It is easy to convince oneself that this condition ensures automatically that the Goldstone theorem is valid, and the  $\pi$  fields remain massless.

Within perturbation theory, the counterterms defined above are power series of the renormalized coupling constant  $\lambda$ . In the  $1/N$  expansion they are power series in  $1/N$ . As it turns out, the contributions to most of these counterterms vanish in the leading order of the  $1/N$  expansion:

$$\Delta\lambda = \delta\lambda^{(0)} + \frac{1}{N}\delta\lambda + \mathcal{O}\left(\frac{1}{N^2}\right)$$

$$Z_\pi = 1 + \frac{1}{N}\delta Z_\pi + \mathcal{O}\left(\frac{1}{N^2}\right)$$

$$Z_\sigma = 1 + \frac{1}{N}\delta Z_\sigma + \mathcal{O}\left(\frac{1}{N^2}\right)$$

$$Z_\chi = 1 + \frac{1}{N}\delta Z_\chi + \mathcal{O}\left(\frac{1}{N^2}\right)$$

$$i(N-1)\alpha^{(0)}(s) = \text{---}\circ\text{---} + \text{counterterm}$$

Figure 1: *The leading order bubble diagram.*

$$\begin{aligned}\Delta t_\sigma &= \frac{1}{N}\delta t_\sigma + \mathcal{O}\left(\frac{1}{N^2}\right) \\ \Delta t_\chi &= \frac{v^2}{N}\delta t_\chi + \mathcal{O}\left(\frac{1}{N^2}\right)\end{aligned}\tag{8}$$

The only counterterm which is needed at leading order in  $1/N$  is actually the  $\delta\lambda^{(0)}$  counterterm of the quartic interaction.

In order to calculate the propagators, one has to evaluate the  $\sigma\sigma$ ,  $\chi\sigma$ ,  $\chi\chi$  and  $\pi\pi$  self-energy diagrams, and then to invert the matrix. As it turns out, the only nontrivial contribution to the proper self-energy functions of the theory in leading order of the  $1/N$  expansion is due to the diagram shown in fig. 1. The ultraviolet divergence of the bubble integral is absorbed in the coupling constant renormalization,  $\delta\lambda^{(0)}$ . One finds the following well-known leading order propagators:

$$\begin{aligned}D_{\sigma\sigma}(s) &= \frac{i}{s - m^2(s)} \\ D_{\chi\chi}(s) &= \frac{1}{Nv^2} \frac{ism^2(s)}{s - m^2(s)} \\ D_{\chi\sigma}(s) &= \frac{1}{\sqrt{N}v} \frac{im^2(s)}{s - m^2(s)} \\ D_{\pi^i\pi^j}(s) &= \delta_{ij} \frac{i}{s}\end{aligned}\tag{9}$$

Here, the quantity  $m^2(s)$  plays the rôle of an energy dependent mass, and is given by the bubble diagram of fig. 1:

$$m^2(s) = \frac{v^2}{\frac{3}{\lambda} + \alpha^{(0)}(s)} \equiv \frac{v^2}{\frac{3}{\lambda} - \frac{1}{32\pi^2} \log\left(-\frac{s+i\epsilon}{\mu^2}\right)}\tag{10}$$

where  $\mu$  is the subtraction scale of the bubble diagram.

We would like to reemphasize that, although a renormalization scale appears in eqns. 9, the physical predictions of this solution are free of any residual renormalization scheme dependence. This is because perturbation theory was summed up in all orders. Whenever one uses this solution of the  $O(N)$  sigma model to relate physical observable quantities, the renormalization scale  $\mu$  can be eliminated from the result. As an example, one can convince oneself that the relation between the Higgs mass and width is independent of the intermediary renormalization scheme used [1].

### 3 Tachyonic regularization

As expected, the propagators  $D_{\sigma\sigma}$ ,  $D_{\chi\chi}$  and  $D_{\chi\sigma}$  derived in the previous section contain a pole corresponding to the Higgs boson. Apart from this, there is of course also a tachyonic pole in these expressions. Its Euclidian position,  $s = -\Lambda_t^2$ , is given by the following equation:

$$\frac{v^2}{\Lambda_t^2} - \frac{1}{32\pi^2} \log\left(\frac{\Lambda_t^2}{\mu^2}\right) + \frac{3}{\lambda} = 0 \quad , \quad (11)$$

and differs from the position of the Landau pole  $\Lambda_L = \mu e^{48\pi^2/\lambda}$  by a correction of order  $v^2/\Lambda_L^2$ . The occurrence of this Euclidian pole creates problems because it spoils the causality of the theory.

Let us analyse the way one performs a calculation in the  $1/N$  expansion. To calculate, let's say, the Higgs propagator, one first performs a double expansion of the self-energy in the coupling constant  $\lambda$  and in  $1/N$ . Then each coefficient in the  $1/N$  expansion is given by a power series in the coupling constant  $\lambda$ . For one given  $1/N$  order, due to the combinatorial structure, one is able to calculate explicitly all Feynman diagrams in the perturbative expansion, and to sum up the  $\lambda$  series. The result then appears to contain an additional tachyonic pole. However, let us notice that the coefficient of the  $1/N$  expansion which we calculate is not defined uniquely by the expansion in  $\lambda$  which we calculate by Feynman diagrams. One still has the freedom to add a function in  $\lambda$  whose perturbative expansion vanishes. Our treatment of the tachyonic pole is based on the observation that its residuum is indeed such a nonperturbative function of the coupling constant, of the type  $e^{1/\lambda}$ . One can add an opposite contribution, so that the tachyonic pole is cancelled, because this contribution vanishes exactly in all orders of perturbation theory.

For this reason, we simply subtract the tachyon minimally at its pole from the leading order propagators. With this prescription, the calculation becomes well-defined, and one can represent the  $O(1/N)$  contribution in terms of a number of Feynman-like graphs. Such a tachyonic regularization can be carried out order by order in the  $1/N$  expansion.

Along the lines of the discussion above, we choose to regularize the propagators of eqns. 9 by subtracting the tachyon pole minimally. We introduce the following subtractions:

$$\begin{aligned} D_{\sigma\sigma}(s) &= i \left( \frac{1}{s - m^2(s)} - \frac{\kappa}{s + \Lambda_t^2} \right) \\ D_{\chi\chi}(s) &= \frac{ism^2(s)}{Nv^2} \left( \frac{1}{s - m^2(s)} - \frac{\kappa}{s + \Lambda_t^2} \right) \\ D_{\chi\sigma}(s) &= \frac{im^2(s)}{\sqrt{N}v} \left( \frac{1}{s - m^2(s)} - \frac{\kappa}{s + \Lambda_t^2} \right) \end{aligned} \quad (12)$$

were

$$\kappa = \frac{1}{1 + \frac{\Lambda_t^2}{32\pi^2 v^2}} \quad (13)$$

is the residuum of the tachyonic pole in the  $\sigma\sigma$  propagator.

It is worthwhile noting in this context that the tachyon not only has a mass of the order of the Landau pole mass. Also its residuum, *i.e.* its coupling to the other fields, is suppressed essentially by the same mass scale. Therefore the effects of the tachyon on the low energy physics are completely negligible as long as the mass of the Landau pole is not very low.

Let us examine the tachyonic regularization of eqns. 12. When we use the tachyonic regularized expressions instead of eqns. 9 for calculating higher order Green function, we essentially modify the Green function by a quantity proportional to  $\kappa$ . As explained, this is a contribution which exactly vanishes in all orders of perturbation theory because  $\kappa$  is a function of the type  $e^{1/\lambda}$ .

Our tachyonic regularization can be seen as a different prescription for summing up the perturbative expansion of a given term in the  $1/N$  expansion. This prescription is such that it does not result in the presence of a tachyon in the theory's spectrum, which would violate causality. At the same time, the original information we started with, that is, the power series in  $\lambda$  of the coefficient of the  $1/N$  expansion, remains untouched. No doubt, this prescription is not unique. For a trivial theory, this ambiguity can be used for modeling the nondecoupling effects associated with unknown physics at a higher energy scale, very much in the same way a cutoff would do. One expects this uncertainty to become important numerically only when the energy of the process under consideration approaches the Landau scale.

Finally, we would like to stress that we do not interpret the tachyonic regularization as a proof that the  $1/N$  expansion is free of tachyons. It only says that within the usual derivation of the  $1/N$  expansion the occurrence of tachyons is arbitrary. To establish conclusively the presence or the absence of tachyons, one needs a procedure for calculating the coefficients of the  $1/N$  expansion without using Feynman diagrams at intermediary stages. Such a procedure is not available so far. Until substantial progress is made in this direction, we prefer a scheme which respects causality and allows one to perform higher order calculations consistently.

## 4 Next-to-leading order calculation

With the tachyonic regularized propagators defined at leading order in the previous section, it is now possible to give a diagrammatic representation of the next-to-leading order contributions to the self-energy functions. The graphs are given in fig. 2. Each graph is in fact an infinite sum of multiloop Feynman diagrams which all are of the same order in the expansion parameter  $1/N$ . This is shown explicitly in fig. 3 for one



$$\begin{aligned}
i\alpha(s) &= \text{---} \begin{array}{c} \bullet \\ \diagup \quad \diagdown \\ \bullet \end{array} \text{---} + \text{---} \begin{array}{c} \bullet \\ \circlearrowleft \\ \bullet \end{array} \text{---} + \text{---} \begin{array}{c} \bullet \\ \triangle \\ \bullet \end{array} \text{---} \\
&\quad A_1 \qquad \qquad \qquad A_2 \qquad \qquad \qquad A_3 \\
&+ \text{---} \begin{array}{c} \bullet \\ \circ \\ \bullet \end{array} \text{---} + \text{---} \begin{array}{c} \bullet \\ \circ \\ \bullet \end{array} \text{---} + \text{counterterms} \\
&\quad A_4 \qquad \qquad \qquad A_5 \\
i\frac{v^2}{N}\beta(s) &= \text{---} \begin{array}{c} \bullet \\ \circlearrowleft \\ \bullet \end{array} \text{---} + \text{---} \begin{array}{c} \bullet \\ \diagup \quad \diagdown \\ \bullet \end{array} \text{---} + \text{counterterms} \\
&\quad B_1 \qquad \qquad \qquad B_2 \\
i\frac{v}{\sqrt{N}}\gamma(s) &= \text{---} \begin{array}{c} \bullet \\ \triangle \\ \bullet \end{array} \text{---} + \text{---} \begin{array}{c} \bullet \\ \circlearrowleft \\ \bullet \end{array} \text{---} + \text{counterterms} \\
&\quad C_1 \qquad \qquad \qquad C_2 \\
i\frac{v^2}{N}\delta(s) &= \text{---} \begin{array}{c} \bullet \\ \circ \\ \bullet \end{array} \text{---} + \text{counterterms} \\
&\quad D
\end{aligned}$$

---●---	= $\chi\chi$
~●---	= $\sigma\chi$
~●~	= $\sigma\sigma$
---	= $\pi\pi$

Figure 2: *Infinite sums of multiloop Feynman diagrams which contribute in next-to-leading order in  $1/N$  to the two-point functions of the  $O(N)$  sigma model. The blob on propagators denotes the summed-up leading order propagators. Note that the  $\pi\pi$  propagator at leading order in  $1/N$  is a free propagator. One of the graphs above is shown in expanded form in fig. 3.*

graph.

With the next-to-leading order self-energy functions defined in fig. 2, it is straightforward to calculate the propagators. In particular, the  $\sigma\sigma$  propagator, which is our main concern in this paper, is given by:

$$D_{\sigma\sigma}^{(NLO)}(s) = \frac{i}{s - m^2{}^{(corr)}(s)} \quad , \quad (14)$$

where

$$m^2{}^{(corr)}(s) = \frac{v^2}{\frac{3}{\lambda} + \alpha^{(0)}(s) + \frac{1}{N} \left\{ -\alpha^{(0)}(s) + \alpha(s) + 2\frac{v^2}{m^2(s)}\gamma(s) + \left[ \frac{v^2}{m^2(s)} \right]^2 \beta(s) \right\}} \quad (15)$$

Because of the complicated form of the expressions, the evaluation of these graphs is highly involved and can only be performed numerically. In order to do the actual calculation new techniques were necessary. We developed techniques which extend the methods of ref. [15] which deals with massive three-loop diagrams. Some graphs are also ultraviolet divergent. It is rather complicated to disentangle the poles in  $\epsilon = n - 4$  of the sets of multiloop diagrams of the type shown in fig. 2. Therefore in

$$iA_1(s) = \text{---} \text{---} \text{---} \text{---} \equiv \sum_{k=0}^{\infty} \sum_{l=0}^{\infty} \text{---} \text{---} \text{---} \text{---}$$

Figure 3: *Multiloop diagrams with three-loop topology which contribute to the  $\chi\chi$  propagator in next-to-leading order.*

order to perform renormalization one first determines the counterterms in terms of multiloop graphs by using the renormalization conditions discussed in the previous section. Then, without evaluating the counterterms explicitly, one adds them to the actual graphs which contribute to the self-energies  $\alpha(s)$ ,  $\beta(s)$ ,  $\gamma(s)$  and  $\delta(s)$ . In the next step, one identifies the divergences and subdivergencies of the graphs, and combines each of them with the appropriate terms of the counterterm contributions at the level of the integrands. In this way one renders each of the graphs ultraviolet finite. One can then apply the numerical methods of ref. [15] for calculating the ultraviolet finite graphs.

At this point it becomes clear that identifying the divergences of the multiloop graphs, choosing an appropriate definition of the counterterms, imposing convenient renormalization conditions, and performing the actual numerical integration are in fact closely related issues. This is rather involved, and we will not enter into such details, which are beyond the scope of this article. We will discuss this in detail in a subsequent publication. Here we only give a sketch of the treatment for one of the graphs.

Let us consider the graph  $A_1$  which is shown in fig. 3. This graph has the topology of a three-loop Feynman diagram, which is the most complicated topology among the graphs of fig. 2. To evaluate this graph, we treat it as if it were a three-loop diagram with two propagators replaced by some more complicated expressions, given by eqns. 12. We evaluate the resulting expression according to ref. [15]. This gives the following two-dimensional integral representation:

$$A_1(s) = \int_{-\infty}^{\infty} dp_0 \int_0^{\infty} d\rho (4\pi\rho^2) D_{\chi\chi}(P_0^2) D_{\chi\chi}(P_k^2) C^2(P_k^2, P_0^2, k^2) \quad , \quad (16)$$

where

$$\begin{aligned} P_0^2 &= p_0^2 - \rho^2 \\ P_k^2 &= p_0^2 + 2p_0\sqrt{k^2} + k^2 - \rho^2 \\ P_\mu^2 &= p_0^2 + 2p_0\mu + \mu^2 - \rho^2 \quad , \end{aligned} \quad (17)$$

and  $k = \sqrt{s}$  is the external momentum of the graph.  $\mu$  is some arbitrary subtraction scale for the subdivergencies of the graph, which will be used in the following.  $C(P_1^2, P_2^2, P_3^2) \equiv C(0, 0, 0; P_1^2, P_2^2, P_3^2)$  is the three-point vertex diagram, for which we use an analytical relation given in ref. [15]. That expression is suitable for our NLO  $1/N$  calculation because it remains on the correct Riemann sheet for the range of parameters needed to evaluate the two-fold integral of eq. 16.

The expression of eq. 16 cannot be evaluated numerically directly because it is ultraviolet divergent. First one has to combine it with the appropriate counterterms in order to subtract its divergencies and subdivergencies, thus rendering this expression finite. After some algebra, and after introducing the notation:

$$\xi = \frac{1}{16\pi^2 P_0^2} \log\left(\frac{s}{\mu^2}\right) , \quad (18)$$

one finds the following subtracted expression:

$$\begin{aligned} A_1(s) = & \int_{-\infty}^{\infty} dp_0 \int_0^{\infty} d\rho (4\pi\rho^2) \times \left\{ D_{xx}(P_0^2) \left[ D_{xx}(P_\mu^2) - D_{xx}(P_0^2) \right] \xi^2 \right. \\ & + D_{xx}(P_0^2) \left[ D_{xx}(P_k^2) - D_{xx}(P_\mu^2) \right] C(P_k^2, P_0^2, k^2)^2 \\ & - 2D_{xx}(P_0^2) D_{xx}(P_\mu^2) \left[ C(P_k^2, P_0^2, k^2) - C(P_\mu^2, P_0^2, \mu^2) + \xi \right] \xi \\ & + 2D_{xx}(P_0^2) D_{xx}(P_\mu^2) \left[ C(P_k^2, P_0^2, k^2) - C(P_\mu^2, P_0^2, \mu^2) + \xi \right] C(P_\mu^2, P_0^2, \mu^2) \\ & \left. + D_{xx}(P_0^2) D_{xx}(P_\mu^2) \left[ C(P_k^2, P_0^2, k^2) - C(P_\mu^2, P_0^2, \mu^2) + \xi \right]^2 \right\} . \quad (19) \end{aligned}$$

Here the subtraction scale of the subdivergencies,  $\mu$ , can be set to zero without encountering any infrared difficulties. This choice is in fact more convenient for the actual calculation. The reader can easily convince himself that the expression above is ultraviolet convergent. The expression can be evaluated numerically fast and precisely by choosing an appropriate complex integration path, as explained in ref. [15].

The other graphs can be evaluated along the same lines. For the graphs  $A_4$  and  $A_5$  we found it advantageous to rewrite the integrands in a special form, which results in a faster algorithm. These methods will be discussed in detail in future publications.

At this point we would like to make some comments related to the renormalization procedure. First, we emphasize again that we use a renormalization scheme at intermediary stages, and a renormalization scale  $\mu$  appears in relations like eq. 19. However, the final physical results are totally independent of this renormalization scheme, just like the leading order results. This is because the perturbation series of the  $1/N$  coefficient is summed up exactly, to all orders.

An interesting effect is that the wave function renormalization constants of the Goldstone and Higgs bosons become finite when calculated in the nonperturbative  $1/N$  expansion. This only shows up nontrivially in the NL order, as there are no contributions to the wave function renormalization constants in leading order. The

reader can easily convince himself that the only graphs potentially giving ultraviolet divergent contributions to the wave function renormalization constants are  $B_1$  and  $D$ . If one considers the Feynman diagrams which are contained in both  $B_1$  and  $D$ , one notices that they are all indeed ultraviolet divergent. However, after summing up all Feynman diagrams which compose these two graphs, the ultraviolet divergency of the wave functions disappears. One is left with very slowly (logarithmical) converging expressions.

The finiteness of wave function renormalization constants is known to be a feature of the exact solution for interacting fields. In fact, one can prove they ought to be numbers with values between 0 and 1. For the truncated perturbative solution this is notoriously not the case, wave function renormalization constants being even ultraviolet divergent in general. For the case of the NLO calculation described here, we were able to prove that the Higgs and Goldstone wave function renormalization constants are finite. However, we could not so far check that their values are between 0 and 1. It is difficult to calculate their actual values numerically because their numerical convergence is only logarithmical and much slower than that of the graphs needed for physical calculations.

The behaviour of higher orders in  $1/N$  is an open question. Still, it is remarkable that the NLO of the  $1/N$  expansion recovers such a property of the exact solution which is absent in perturbation theory.

## 5 Nonperturbative Higgs lineshape

The Higgs propagator which we calculated in the previous section is essentially a physical quantity. It can in principle be measured in a fermion scattering process, for instance the  $\mu\bar{\mu} \rightarrow t\bar{t}$  process, which is relevant for muon collider studies. The only contribution which one still has to add is the correction to the two Yukawa couplings of the Higgs to the fermions. As long as one only considers the contributions of leading order in the mass of the fermions, it is well-known [12, 13, 14] that these contributions are energy independent, and are simply given by the ratio of the wave function renormalization constants of the Higgs and the Goldstone bosons. Regarding the evaluation of this ratio, we already mentioned in the previous section that  $Z_\sigma$  and  $Z_\pi$  are both finite at NLO in  $1/N$ , but evaluating them separately is very difficult because they converge very slowly. However, they have the same ultraviolet behaviour and for this reason their ratio is well-behaved numerically. In this context one can note that this ratio is ultraviolet finite even in perturbation theory.

The results for the lineshapes are given in fig. 4. We plot the lineshape function  $f(\sqrt{s}) = |D_{\sigma\sigma}(s)Z_{\sigma\sigma}^2/Z_{\pi\pi}^2|^2$ , both at LO and at NLO in the  $1/N$  expansion. We also compare with the known perturbative results up to NNLO [16]. For the purpose of comparing the predictions of perturbation theory and of the  $1/N$  expansion, we compare in fig. 4 Higgs lineshapes which have the same position of the peak.

As one can see, there is a substantial discrepancy between the  $1/N$  expansion in

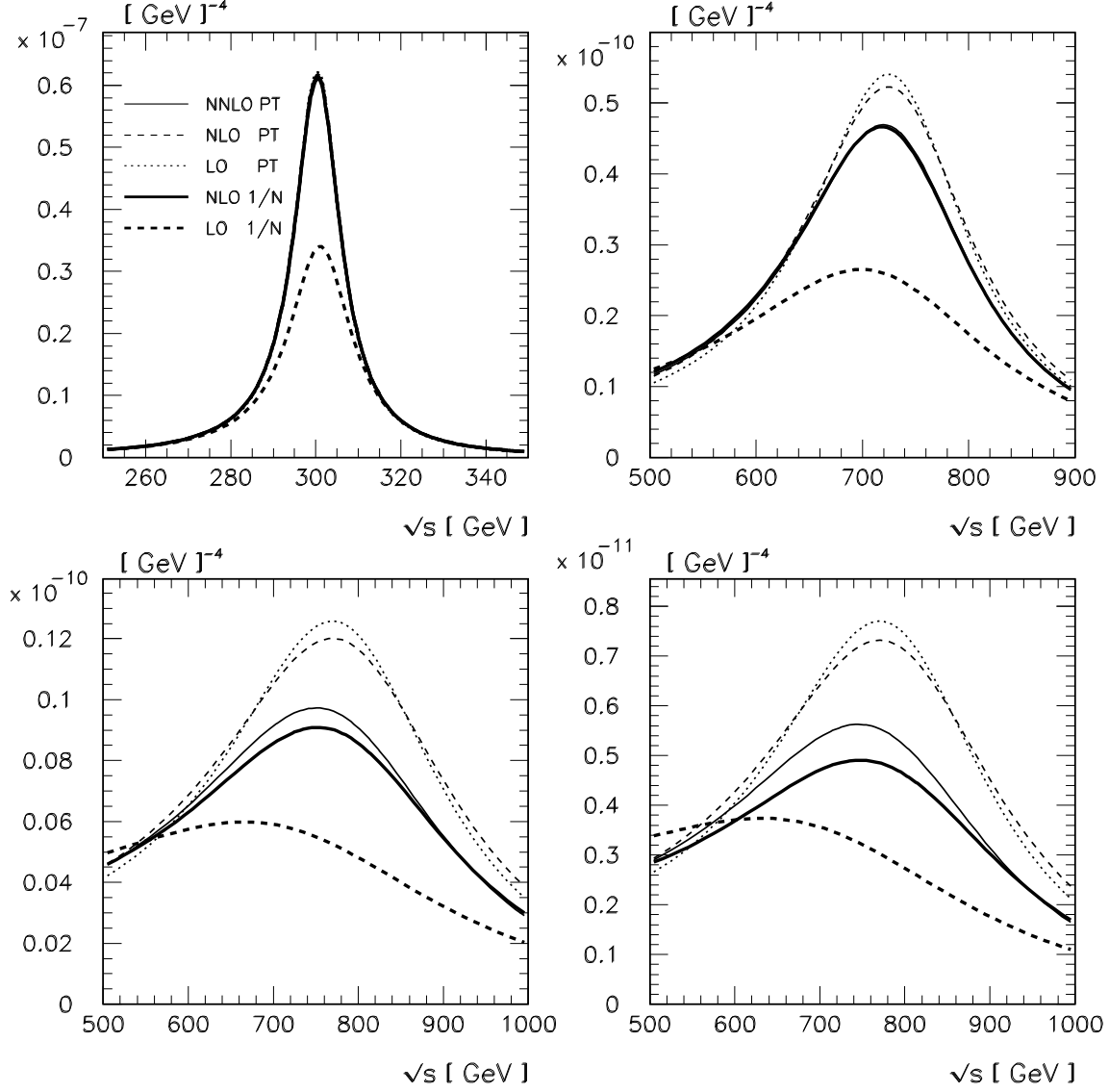


Figure 4: *The Higgs lineshape in fermion scattering. Comparison between the perturbative lineshape (LO, NLO, NNLO) and the nonperturbative 1/N expansion (LO, NLO) for different values of the coupling. We compare lineshapes so that the position of the peak in two-loop perturbation theory and NLO 1/N expansion is the same. The lineshapes in NNLO perturbation theory and NLO 1/N are almost indistinguishable up to about 700 GeV.*

leading order and perturbation theory even for low values of the coupling. We notice that our NLO result lies between the perturbative results and the lowest order in  $1/N$ . The corrections are actually quite large compared to the lowest order in  $1/N$ . For low coupling we see that one is very close to perturbation theory now, which indicates that we should have a good approximation for the Higgs line shape. For Higgs masses larger than about 850 GeV there is a fairly large difference between perturbation theory and the  $1/N$  expansion. Perturbation theory is probably not reliable anymore, but things seem to be converging.

For even larger values of the coupling the behaviour of the  $1/N$  solution and of perturbation theory becomes different, and lineshapes cannot be compared at the same position of the peak any longer. This behaviour can be seen in fig. 5. Here we plot lineshapes in NLO  $1/N$  expansion and in two-loop perturbation theory for a range of couplings. Since perturbation theory breaks down for large couplings, the perturbative plots for heavy Higgs bosons are given only for comparison purposes. While the position of the peak in perturbation theory increases continuously with the coupling, the  $1/N$  solution shows a saturation around 930 GeV, after which only the decay width continues to increase.

In order to study this in somewhat more detail, we plotted in fig. 6 two observable quantities which can be interpreted as an effective Higgs mass and width. Here, ideally one would like to plot instead the real and the imaginary part of the pole of the Higgs propagator because they are universal for all Green functions and are not process dependent. However our numerical programs do not allow us at the moment to calculate the graphs on the second Riemann sheet and solve the pole equation.

Therefore we use a procedure to define an effective mass  $M_{peak}$  and width  $\Gamma_{peak}$  from the lineshape itself, which is more directly related to experiment. The mass  $M_{peak}$  is defined as the location of the peak of the cross section. The width  $\Gamma_{peak}$  is taken from the peak height of the cross section as if the lineshape was determined by a resonant Higgs propagator only, giving rise to a Breit–Wigner shape:

$$\sigma(s) \sim \frac{1}{(s - M_{peak})^2 + M_{peak}^2 \Gamma_{peak}^2} . \quad (20)$$

Of course, the lineshape is not exactly a Breit–Wigner resonance. However, we found that this definition of the width is within a few percent of for instance the width at half–maximum. The description by  $M_{peak}$  and  $\Gamma_{peak}$  gives therefore a satisfactory approximation of the leading features of the Higgs lineshape. It should be good enough to be used as a first approximation for phenomenological applications.

Our results can strictly speaking not be used directly at the LHC. This is because one should also take higher order  $1/N$  correction in the Higgs–Goldstone boson vertex into account. However, we expect that the correction to the width will be the dominant feature in practice. For values of the Higgs mass larger than about 900 GeV, the saturation effect sets in, and the uncertainty due to the discrepancy between the perturbative and the  $1/N$  widths becomes important. The Higgs becomes wider, and

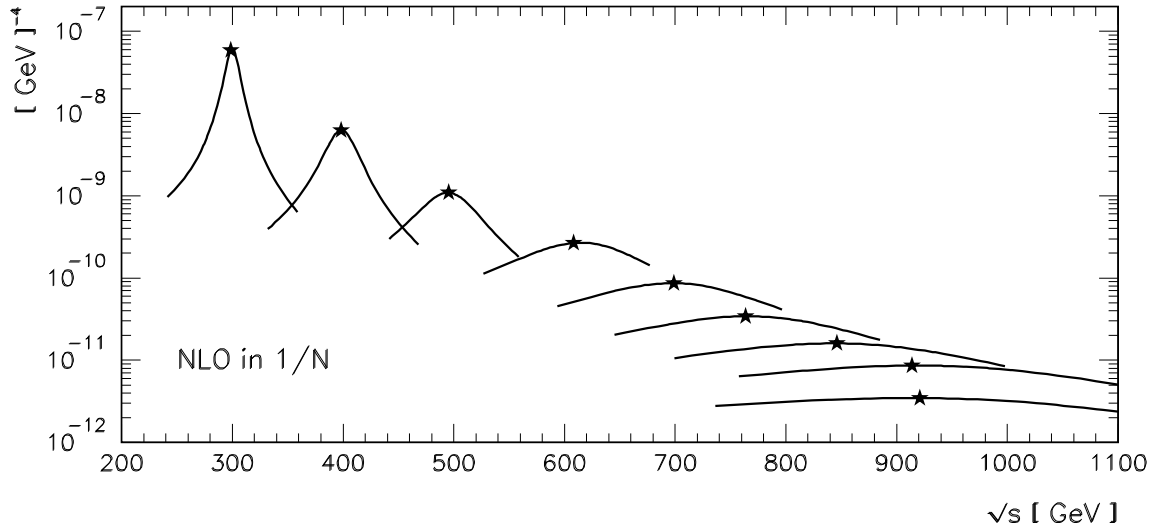
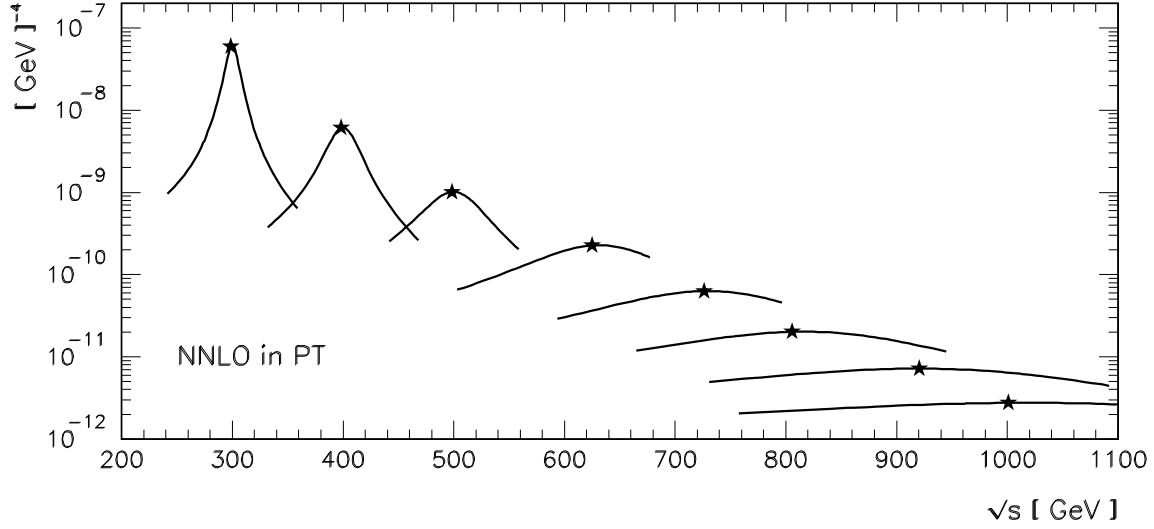


Figure 5: *Higgs lineshapes in perturbation theory (two-loop) and in the nonperturbative  $1/N$  expansion (NLO), where we marked the position of the peak. One can see the saturation of the position of the peak for large values of the coupling.*

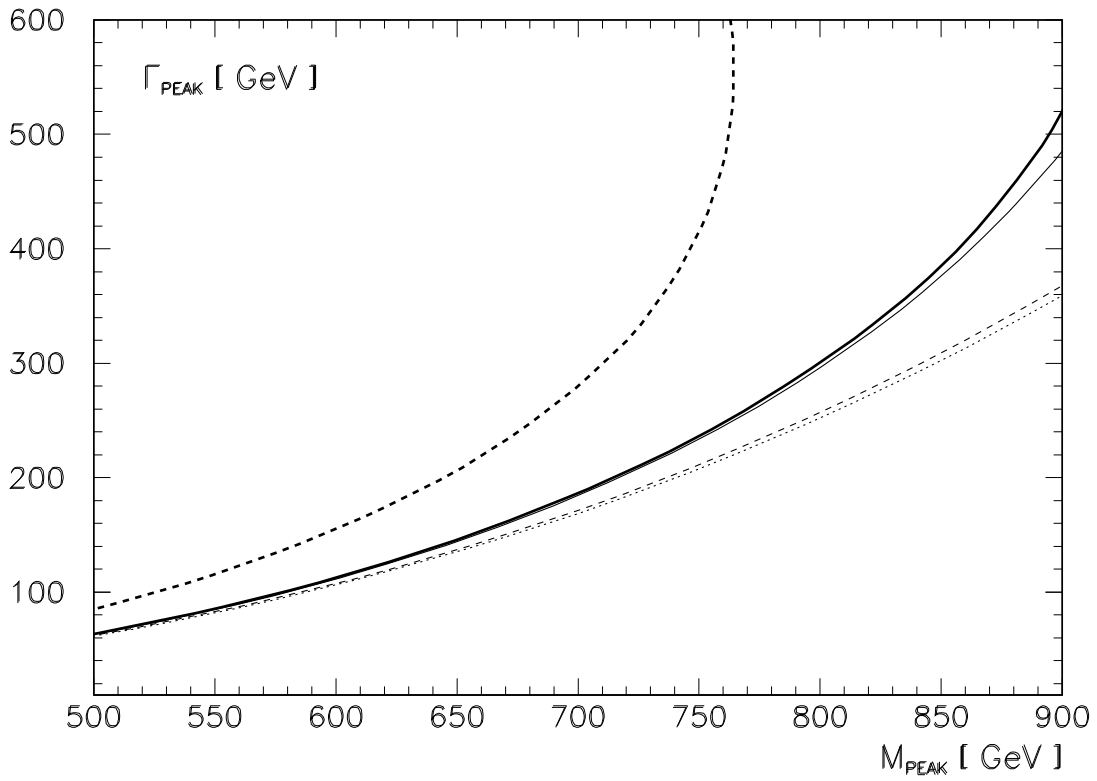
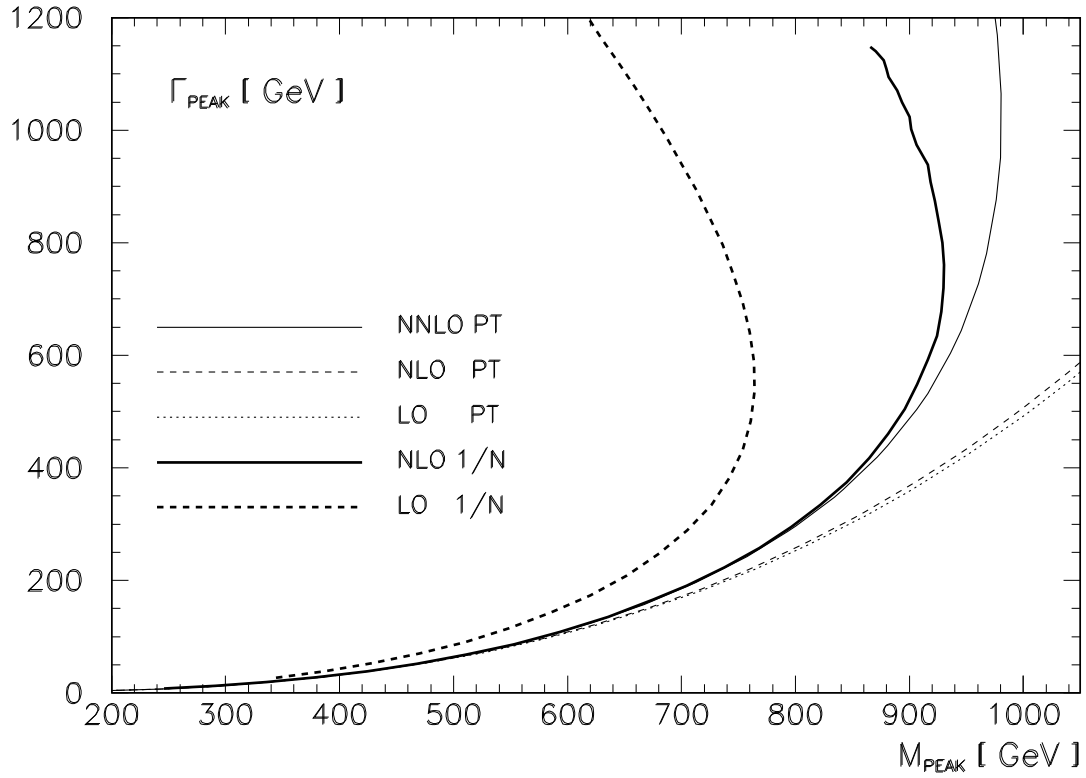


Figure 6: *The relation between the peak variables  $M_{PEAK}$  and  $\Gamma_{PEAK}$  in perturbation theory and in the  $1/N$  expansion.*



the signal is washed out and lost in the background. This saturation effect can be quite important for LHC physics and the discovery limits there.

We plot in fig. 6 the effective width  $\Gamma_{peak}$  as a function of  $M_{peak}$  both in the  $1/N$  expansion and in perturbation theory. One can see from fig. 6 that the  $1/N$  expansion and perturbation theory appear to be converging towards a common relation between the Higgs width and mass. For a Higgs mass up to about 850 GeV, the agreement is remarkable. Afterwards the numerical values start to deviate. The nonperturbative width is larger than the width in perturbation theory, and saturation sets in. A maximum of the effective Higgs mass appears at around 930 GeV.

For phenomenological purposes we give in the following a simple approximate formula to relate  $M_{peak}$  and  $\Gamma_{peak}$ . Expressing  $M_{peak}$  and  $\Gamma_{peak}$  in TeV, one can use the following relation:

$$M_{peak}^3 = 2.02582 \cdot \Gamma_{peak} - 0.812725 \cdot \Gamma_{peak}^2 - 1.01729 \cdot \Gamma_{peak}^3 + 0.541511 \cdot \Gamma_{peak}^4, \quad (21)$$

which is simply a fit of the NLO  $1/N$  curve shown in fig. 6. Its precision is at the per mille level for the range of couplings shown in fig. 6. For comparison, the corresponding fit for the two-loop perturbative curve is the following (the exact two-loop lineshape is given in ref. [16]):

$$M_{peak}^3 = 2.09069 \cdot \Gamma_{peak} - 1.23887 \cdot \Gamma_{peak}^2 - 0.0233177 \cdot \Gamma_{peak}^3 + 0.115571 \cdot \Gamma_{peak}^4. \quad (22)$$

## 6 Conclusions

We treated an  $O(N)$ -symmetrical sigma model with spontaneous symmetry breaking in the nonperturbative  $1/N$  expansion at next-to-leading order.

In order to calculate corrections of higher order in  $1/N$  one needs a prescription for the treatment of the tachyons which appear in the propagators at leading order. We showed that in the usual derivation of the  $1/N$  expansion the occurrence of tachyons is arbitrary, and it can be eliminated when one realizes that the coefficient of the  $1/N$  expansion is only determined up to a function of the coupling constant which vanishes identically in perturbation theory. Therefore we introduced a scheme of tachyonic regularization which can be performed consistently order by order in the  $1/N$  expansion. Our tachyonic regularization can be interpreted as a prescription for the summation of the coefficient of the  $1/N$  expansion which leaves unchanged its perturbative expansion and preserves causality at the same time.

The tachyonic regularization is not unique. This arbitrariness can be used for modelling nondecoupling effects of unknown physics at a higher energy scale. This arbitrariness is an interesting problem which deserves further investigation.

We then developed techniques to calculate infinite sets of multiloop Feynman diagrams which are needed for higher order calculations in  $1/N$ . We applied these techniques to the Higgs sector of the standard model,  $N = 4$ , and calculated the Higgs propagator and the lineshape of the Higgs resonance at muon colliders. The results are interesting, and confirm qualitatively some results obtained previously based on the leading order solution, such as the saturation of the Higgs mass. In NLO, it occurs at a value of about 930 GeV. Moreover, compared to the leading order, the NLO correction is rather substantial. It leads for low couplings to a remarkable agreement between perturbation theory and  $1/N$  expansion, thus solving a long-standing puzzle. This agreement proves that the nonperturbative  $1/N$  expansion in higher orders, when combined with the tachyonic regularization, is a useful tool for treating strong couplings. It can give very precise results.

Our NLO solution has certain properties associated with a nonperturbative solution. For instance, it contains no residual renormalization scheme dependence. Of course, this is true for the leading order as well. An interesting property which only shows up at NLO is the finiteness of wave function renormalization constants, which also ought to be satisfied by the exact solution, and which does not hold in perturbation theory.

Regarding Higgs searches at future colliders, it is interesting that the perturbative two-loop correction is substantial when compared to the one-loop and tree level, but turns out to be close to the nonperturbative solution which we derived up to about 900 GeV. This reduces drastically the theoretical uncertainty of a heavy Higgs width.

For larger couplings, our results show a deviation from perturbation theory. Essentially, the Higgs width is always larger than in perturbation theory. The Higgs mass is saturated, and its width can grow without its mass becoming larger at the same time. This effect must be taken into account in view of heavy Higgs searches at LHC. For phenomenological purposes we gave a simple approximate formula to relate the Higgs mass and width which is valid for large couplings as well.

### Acknowledgements

We would like to thank George Jikia and Boris Kastening for discussions. The work of A. G. was supported by the Deutsche Forschungsgemeinschaft (DFG).

## References

- [1] M.B. Einhorn, *Nucl. Phys.* **B246** (1984) 75.
- [2] R. Casalbuoni, D. Dominici, R. Gatto, *Phys. Lett.* **B147** (1984) 419.
- [3] J.P. Nunes, H.J. Schnitzer, *Int. J. Mod. Phys.* **A10** (1995) 719.
- [4] W. Bardeen, M. Moshe, *Phys. Rev.* **D28** (1983) 1372.

- [5] R. Haymaker, *Phys. Rev.* **D13** (1976) 968.
- [6] M. Kobayashi, T. Kugo, *Prog. Th. Phys.* **54** (1975) 1537.
- [7] L.F. Abbott, J. Kang, H.J. Schnitzer, *Phys. Rev.* **D13** (1976) 2212.
- [8] R.G. Root, *Phys. Rev.* **D10** (1974) 3322; *Phys. Rev.* **D11** (1975) 831; *Phys. Rev.* **D12** (1975) 448.
- [9] L. Dolan and R. Jackiw, *Phys. Rev.* **D9** (1974) 3320.
- [10] H.J. Schnitzer, *Phys. Rev.* **D10** (1974) 1800.
- [11] S. Coleman, R. Jackiw, H.D. Politzer, *Phys. Rev.* **D10** (1974) 2491.
- [12] A. Ghinculov, *Nucl. Phys.* **B455** (1995) 21. A. Ghinculov, *Phys. Lett.* **B337** (1994) 137; (E) **B346** (1995) 426. A. Ghinculov and J.J. van der Bij, *Nucl. Phys.* **B436** (1995) 30.
- [13] A. Frink, B.A. Kniehl, D. Kreimer, K. Riesselmann, *Phys. Rev.* **D54** (1996) 4548. L. Durand, B.A. Kniehl and K. Riesselmann, *Phys. Rev.* **D51** (1995) 5007; *Phys. Rev. Lett.* **72** (1994) 2534; (E) *Phys. Rev. Lett.* **74** (1995) 1699.
- [14] V. Borodulin and G. Jikia, *Phys. Lett.* **B391** (1997) 434.
- [15] A. Ghinculov, *Phys. Lett.* **B385** (1996) 279.
- [16] T. Binoth and A. Ghinculov, *Phys. Rev.* **D56** (1997) 3147.